Journal of Cleaner Production 434 (2024) 140316

Contents lists available at ScienceDirect

Journal of Cleaner Production

journal homepage: www.elsevier.com/locate/jclepro

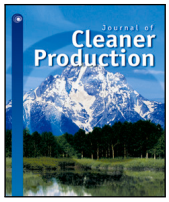

Assessment of heat and entropy balance of an OWC wave energy converter

A. Molina-Salas [a,*], Rami Hatafi [b], F. Huertas-Fernández [a], M. Clavero [a], A. Moñino [a]

[a] Andalusian Institute for Earth System Research, University of Granada, Av. del Mediterráneo s/n, 18006, Granada, Spain
[b] INSA Lyon, Department of Energy and Environmental Engineering, 20 Avenue Albert Einstein, 69621 Villeurbanne Cedex, France

ARTICLE INFO

Handling Editor: Jin-Kuk Kim

Keywords:
Wave energy converter (WEC)
Oscillating water column (OWC)
Thermodynamics
Polytropic process
Entropy
Emergy

ABSTRACT

This paper deals with the thermodynamic processes governing an Oscillating Water Column (OWC) device, focusing on the entropy variation and the energy and heat budgets over the expansion–compression cycles. The influence of the thermodynamic performance on the Levelized Cost of Energy (LCOE) and the carbon footprint is analysed. The research deals with an experimental research on a simple OWC off-shore model for the purpose, with the open gas system inside the chamber formulated by a real gas model, and conceptually represented by an equivalent closed one in order to apply the First Principle of Thermodynamics appropriately. Analysed results show that the compression process is an *active* process, while the expansion process is a *passive* one. In addition, the observed non-adiabatic performance of the complete cycle implies a efficiency reduction, with consequences on the LCOE. Furthermore, an approach to emergy (embodied energy) analysis is considered, providing with concluding remarks on OWC renewability and possible impacts on the biosphere and GHG emissions. An utter approach on OWC energy and emergy assessment will be develop on future researches.

1. Introduction

The oscillating water column (hereinafter OWC) is probably one of the wave energy conversion technologies (hereinafter WEC) which has received more attention from researchers in the past decades, Falcão and Henriques (2016), SI Ocean (2012), Falcão (2010), Cruz (2008), The Carbon Trust (2005). The OWC design concept essentially consists of a partially submerged air chamber, opened at the bottom to allow wave action on the inner air storage volume and connected at the top to a turbine duct and a generator. From that concept, the OWC problem is developed and solved within the framework of Linear Theory under a radiation–diffraction focusing, Evans (1982), Sarmento and Falcão (1985), Evans and Porter (1995), Martins-Rivas and Mei (2009).

OWC power plants have been designed and implemented worldwide, with outstanding pilot project facilities such as PICO (Portugal, installed capacity 400 kW, Falcão et al. (2020)) or Mutriku (Spain, installed capacity 296 kW, Torre-Enciso et al. (2009), Gabriel Ibarra-Berastegi et al. (2018)) to cite some examples within a wide list, The Carbon Trust (2005). Whether those plants have completed their service lifetime or remain as test rigs to advance in research and development, a key factor is that those plants can be considered as benchmarks both in terms of wave energy farming full commissioning guidelines and of valuable data sources for ongoing research lines, for instance Gato et al. (2022).

The challenges involving the design and commissioning of full scale pilot plants reveal the main scientific and technical problems have been circumvented, hence all major obstacles regarding wave impingement, primary capture and transformation, pneumatic compression/expansion, turbine performance and delivery of electricity to the grid have been solved indeed. However, research is necessary to assess governing factors in OWC performance, so ensuring advances in terms of feasibility of implementation under general conditions (SI Ocean, 2013), levelized cost of energy (hereinafter LCOE), de Andres et al. (2017), and renewability efficiency, de Oliveira (2013), Molina-Salas et al. (2022b).

In the line of balancing investment trough capital and operative expenses (hereinafter CAPEX and OPEX), energy farming annual energy production (hereinafter AEP), levelized cost of energy and project depreciation, OWC research advances in recent years have aimed to the feasibility of commissioning OWC projects to cope with wave energy objectives, Magagna and Uihlein (2015), Uihlein and Magagna (2015), O'Hagan et al. (2016). Authors have analysed the implementation of OWC converters as part of maritime structures, Boccotti et al. (2007), Mendoza et al. (2017), Simonetti and Cappietti (2021), Fox et al. (2021), to apply the OWC technology as an additional feature in coastal protection, Mendoza et al. (2014), Abanades et al. (2014c,a,b), Medina-López et al. (2017a), Bergillos et al. (2018), or to apply the primary

* Corresponding author.
E-mail address: amsalas@ugr.es (A. Molina-Salas).

https://doi.org/10.1016/j.jclepro.2023.140316
Received 18 October 2023; Received in revised form 6 December 2023; Accepted 18 December 2023
Available online 21 December 2023

List of Symbols

Latin symbols

A_b	Turbine blades area (m^2)
A_t	Total cross section area occupied by the blades (m^2)
B	Second virial coefficient (–)
C_p	Specific heat under constant pressure (J/mok K)
C_p^*	Specific heat under constant pressure for the ideal gas (J/mok K)
C_v	Specific heat under constant volume (J/mok K)
C_v^*	Specific heat under constant volume for the ideal gas (J/mok K)
C_y	Specific heat under constant state equation y (J/mok K)
D_{int}	Internal turbine diameter (m)
D_{OWC}	Internal OWC device diameter (m)
D_t	External turbine diameter (m)
E	Total energy of the air system inside the chamber (J)
E'	Total energy of the air system outside the chamber (J)
e_{da}	Needed exergy to the deactivation of possible generated waste in the process (J/mol)
e_{dp}	Exergy rate related to waste disposal of the process (J/mol)
e_{dt}	Destroyed exergy in the complete process (J/mol)
e_{em}	Exergy of the wastes that are emitted to the atmosphere (J/mol)
e_{nr}	Exergy of non-renewable fuel (J/mol)
e_{out}	Exergy of the products (J/mol)
F	Emergy assigned to purchased feedback flows of goods and human services from economy (seJ)
f_0, f_1, f_2	Temperature correlation functions (–)
g	Gravitational acceleration (m/s^2)
H	Enthalpy (J)
H_s	Wave height (m)
h	Specific enthalpy (J/kg)
h^*	Specific enthalpy for the ideal gas (J/kg)
h_w	Water depth (m)
kh	Relative depth (–)
L_{piston}	Deformation work at the piston (J)
L_{sys}	External work performed at the boundary by the OWC system - (J)
L_{total}	Total work performed by the system (J)
l	Specific work (J/kg)
M	Molar weight (kg/mol)
m	Polytropic index (–)
m	Air mass inside the chamber (kg)
m'	Air mass outside the chamber (kg)
N	Turbine rotation velocity (rad/s)
N	Emergy assigned to non-renewable sources (seJ)
n	Polytropic exponent (–)
p	Air pressure inside the chamber (Pa)
p'	Air pressure outside the chamber (Pa)
Q	Heat (J)
Q^m	air flow rate (kg/s)
Q_{OWC}	Volumetric flow rate at the turbine inlet (m^3/s)
q	Specific heat (J/kg)
R	Emergy assigned to renewable sources (seJ)
$R_0 = 8.31$ J/K mol	Universal gas constant
r_W	Ratio between the power output of the full-scale OWC device and the OWC scaled device (–)
S	Entropy (J/K)
s	Specific entropy (J/kgK)
s^*	Specific entropy for the ideal gas (J/molK)
T	Temperature (K)
T'	Temperature outside the chamber (K)
T_z	Wave period (s)
U	Internal energy of the air system inside the chamber (J)
U'	Internal energy of the air system outside the chamber (J)
u	Specific internal energy of the system (J/kg)
u^*	Specific internal energy for the ideal gas (J/kg)
V	Air volume inside the chamber (m^3)
V'	Air volume outside the chamber (m^3)
v	Flow velocity along turbine axis direction (m/s)
$v_m = V/N$	Molar volume of gas (m^3/mol)
Y	Emergy assigned to the output production system (seJ)
y	Auxiliary variable
Z	Compressibility factor (–)
z	Generic height (m)

Greek symbols

η	Isentropic efficiency (–)
η_{ex}	Exergy efficiency (–)
λ	Geometric scale ratio (–)
λ_{em}	Emergy renewability index (–)
λ_{ex}	Exergy renewability index (–)
μ	Chemical potential (J/mol)
σ	Turbine solidity (–)
χ_{mol}	Molar fraction of vapour in dry air
ω	Acentric factor (–)

wave energy conversion to secondary transformation such as hydrogen production, Huertas-Fernández et al. (2021). With the aim to reduce the capital expenses, some researches are focused on combining the OWC technology with other electricity production systems, like wind energy systems or other wave energy converters, Fenu et al. (2023), Wan et al. (2023), or by using floating OWC devices, Portillo et al. (2023). Other authors are focused on improving the annual energy production by improving the turbine performance, Morais et al. (2023), Torres et al. (2018), Setoguchi et al. (2004).

One key factors in OWC operation is the pressure changes induced by wave action in the air system inside the chamber – compression and expansion –, driving the turbine and inducing the readjustment of the instantaneous pressure response of the system, and so on, in a feedback process that can be approached as a spring-like air compressibility effect, even if the air can be considered as incompressible

Abbreviations

AEP	Annual electricity production (MWh)
$CAPEX$	Capital expenditures (£)
$const$	constant.
EIS	Emergy index of sustainability (–)
$LCOE$	Levelised Cost of Energy (€/MWh)
NPV	Net Present Value (–)
$OPEX$	Operational expenditures (£)
OWC	Oscillating Water Column.
RH	Relative humidity (–)

for the velocity range to be expected inside the chamber. In fact the radiation–diffraction problem is the formal representation of that process, considered as the superimposition of a diffraction field from wave impingement in which the pressure inside the chamber is fixed, and a radiation field induced by a pressure fluctuation under static water condition, as adequately proposed in Sarmento et al. (1990). The key factor in the interpretation of the radiation–diffraction problem, and more specifically in the spring-like air compressibility effect, is that the compression/expansion process undergone by the gas inside the chamber strictly follows a general polytropic process equation for a simple closed system, relating pressure p and volume V through the polytropic exponent n in the form $pV^n = const$, Moñino et al. (2020). Both the conditions supporting the hypothesis of simple closed system and the specific nature of the process to be described by n, will be discussed later. For any water surface elevation state throughout each wave cycle, the instantaneous air pressure inside the chamber is unequivocaly related with its corresponding volume through the process equation. In other words, at every time step the system is taken to a specific state (p, V) given by the process equation. In consequence, any change in the conditions will lead to a mismatch between p and V, to a readjustment between pressure and volume and to a perturbation in the water surface elevation to be scattered back through all the water column. It is clear that the conditions under which pressure is observed, i.e. temperature and humidity, as well as the turbine type and the solidity, or any other implementation such as the replacement of the turbine by a duct of reduced diameter for example, may have a noticeable influence in the compression/expansion cycle and in the calculation of thermodynamic state variables.

The study of the compression/expansion thermodynamics and the air exchange between the chamber and the outer region presents difficulties both in terms of formulation and observation. Influencing factors such as deviations from pure adiabatic process, open system considerations, effects of turbine characteristics, operating conditions other than ideal dry air hypothesis and governing effect of moisture, make it difficult to retrieve accurate information under specific conditions from the analytical solutions of the radiation–diffraction problem solely. In that sense OWC experimentation, which is also addressed in the methodology of the present research, can provide with an improved insight on thermodynamic processes. Authors have advanced in the study of the similarity requirements for the enhancement of OWC model test results, Falcão and Henriques (2014). Laboratory research has been conducted on the sensibility of OWC performance to air compressibility, López et al. (2020). Research has been recently developed to improve the analysis of OWC experimental data, by means of theoretical corrections accounting for compressibility effects that can be difficult to interpret when comparing between model and prototype, Falcão et al. (2022). In addition, scale effects have to be accounted in order to conduct a correct interpretation of OWC experimental results, Weber (2007), Dimakopoulos et al. (2017).

One of the governing factors concerning the OWC efficiency is the mutual interaction involving the thermodynamics of the OWC chamber and the turbine performance. The thermodynamics of the OWC chamber and the air spring-like effect are object of up-to-date research. Authors have approached the thermodynamic problem assuming an ideal gas undergoing an adiabatic process, Falcão and Justino (1999), Sheng et al. (2013), Sheng and Lewis (2016). Further comprehensive discussions have been presented, analysing the adiabatic condition during compression cycle and the general polytropic performance during expansion, Falcão and Henriques (2019). In addition, the implementation of a real gas model in the radiation–diffraction problem under a relaxation of the adiabatic process condition, has revealed that variations in the air density induced by moisture can led to deviations in pneumatic power and entropy, Medina-López et al. (2017b, 2019), with effects on performance that might also help to explain the otherwise low efficiency values reported when available, The Carbon Trust (2005). In fact, recent experiments in wind tunnel designed to set comprehensive boundaries to the compression process, have shown the turbine itself operates as a restraint for the thermodynamic system inside the chamber, in which the air–water vapour mixture responds to a polytropic exponent that may deviate from the ideal/adiabatic condition, Molina-Salas et al. (2022a). Whether the effect of those conditions might be more or less noticeable depending on wave climate and ambient conditions, Gonçalves and Teixeira (2022), the fact is that the influence over operating cycles might be not negligible, Molina-Salas et al. (2022b), thus affecting LCOE estimates and cost-effective design.

Pressure and temperature – and humidity in the case of air–water vapour mixture hypothesis as part of a real gas model implementation – plays a fundamental role when calculating thermodynamic state variables. State variables provide with key information on thermodynamic performance of the OWC, utterly necessary to set operative ranges, mass and energy exchanges with the surroundings and optimum efficiency in terms of deviation from adiabatic ideal conditions – for which maximum efficiency is to be expected, Falcão and Henriques (2014) –. More specifically, enthalpy and entropy are governing state variables in the analysis of the thermodynamics of compression and expansion cycles, and in the formulation of the heat flow over the complete process. In fact, entropy is the fundamental state variable in the exergy budget. Exergy analysis provides with a comprehensive description of energy balance and mechanical work from primary conversion to final transformation stages such as hydrogen production, Huertas-Fernández et al. (2021). In addition, exergy is directly related with the LCOE not only through the global efficiency of the OWC converter, but also with the renewability in formal thermodynamic terms, de Oliveira (2013), Molina-Salas et al. (2022b), and with the carbon footprint.

The objective of this research is to conduct and comprehensive study of the entropy cycle over compression and expansion processes during OWC operation, and to assess the energy and heat budgets from the standpoint of reversibility, ultimately related with OWC efficiency and renewability, and consequently, with the Levelized Cost of Energy and the carbon footprint. An experimental methodology with a simple OWC off-shore model is addressed for the purpose, on the basis of the thermodynamic formulation in which a real gas model is implemented.

The paper is organized as follows. First, Thermodynamics background of open system process and its adaption to closed system is developed. Afterwards, experimental setup description and methodology are presented, including model description of OWC chamber and turbine, and tests configuration details. Finally, results, analysis and further discussion are presented, with conclusions and possible future research.

2. Thermodynamics

2.1. Open system Thermodynamics and the First Principle

The formulation of the First Principle of Thermodynamics requires the consideration of a closed system. In order to apply the First Principle to an open system, i.e. an OWC converter, the system has to

be *transformed* into a closed one. A comprehensive discussion on the subject is developed in Kestin (1966) and followed up in Falcão and Justino (1999), Josset and Clément (2007), which is addressed in all the background of the present research.

In fact a fictional closed system built in that way ensures the consideration of system functions governing thermodynamic equilibrium states without loss of accuracy. One feasible way to build a closed system from an open one is to add piston devices to its entrance and exit respectively, so that the fluids at entrance and exit can be considered as closed and in equilibrium under their respective piston devices action. Another way to consider a closed system condition is to select an eventually mobile and deformable control volume and the closed system it encloses, and track all the transformation it undergoes from the entrance to the exit. While the first concept represents an *Eulerian* focusing, the second one implies a *Lagrangian* point of view. The last one underlies the theoretical background in Moñino et al. (2020).

Taking as an example the OWC device and focusing on the Eulerian framework, the transformation of the OWC open system into a fictional closed one is sketched in Fig. 1. The OWC system consists of a gas mass m in a thermodynamic equilibrium state described by its total energy E, internal energy U and pressure, volume and temperature (p, V, T). The outside ambient condition is set by a piston device with an infinitely slow motion that ensures equilibrium state in the gas mass m', represented by its total energy E', internal energy U' and pressure, volume and temperature (p', V', T'). The wave action on the system inside the OWC chamber is represented by an eventually deformable contour through which it takes place the exchange of heat Q and deformation work $Lsys$ – the compression/expansion wave action on the gas inside the chamber –. There is no need to represent the wave action by a piston actuator since there is no gas mass exchange though the gas–water interface, and the deformation work itself can be determined through the radiation–diffraction theory and the thermodynamic formalism. As a mass $\delta m'$ is forced inside the OWC system during the OWC expansion cycle for example, the mass m inside the OWC and $\delta m'$ will undergo an equilibrium balance of temperature as part of the mixing process, and it is feasible to consider that there is no heat exchange between masses and that the final state $m + \delta m'$ is instantly uniform inside the OWC chamber. Hence, the closed system evolves between initial and final states of equilibrium, with a mass $\delta m'$ added to the OWC system, exchanging during the process a quantity of heat and work through the contour, and performing a quantity of work at the piston. From the scope of the closed system, the initial state comprises two subsystems, the OWC chamber in equilibrium with the wave action – formerly the open subsystem – and the gas in equilibrium with the piston, while the final state is represented by the mixture of both. An equivalent situation would take place during OWC compression. In this situation, the piston is acting as a manostat and a thermostat, keeping the pressure and temperature of the external subsystem constant and equal to the atmospheric values.

With the previous considerations, the First Principle states that the heat exchanged through the process equals the balance between total energy variation from initial to final state, and the work performed by the system:

$$\delta Q = \delta E_{total} + \delta L_{total} \tag{1}$$

The sign in the right hand of Eq. (1) is chosen to be consistent with the rationale in Kestin (1966), i.e. mechanical work done by the system positive and heat radiated by the system positive—. The First Principle so expressed brings to front the fact that the heat exchanged by the system during a certain process represents the difference between energy content and work required to evolve from initial to final state. Whether the heat is rejected or received, it depends on the nature of the total work performed on/by the system.

The total energy of the closed system at initial and final states can be expressed as:

$$\begin{aligned} E_{ini} &= E + \delta E' = E + e'\delta m' \\ E_{final} &= E + \delta E \end{aligned} \tag{2}$$

where E = energy of the OWC system, $\delta E'$ = energy of the mass $\delta m'$ previous to mixing which can be ultimately expressed in terms of its specific energy e', δE = energy variation in the OWC system at final state. Hence:

$$\delta E_{total} = E_{final} - E_{ini} = \delta E - \delta E' \tag{3}$$

The total work performed by the system is the sum of the external work δL_{sys} performed at the boundary by the OWC system – the sign yet to be determined regarding compression/expansion – and the deformation work at the piston:

$$\delta L_{total} = \delta L_{sys} + \delta L_{piston} = \delta L_{sys} - p'\delta V' \tag{4}$$

Substituting δE_{total} and δL_{total} in (1):

$$\delta Q = \delta E - \delta E' + \delta L_{sys} - p'\delta V' \tag{5}$$

The most general expression of the energy of a system includes internal, kinetic, potential and chemical components. However, when the processes governing the system are deformation work at contours and/or pistons, the effects of kinetic and potential energy, as well as the chemical potential, can be neglected. In the case of the energy variation δE for the closed system at the final state, it can be simplified to:

$$\delta E \simeq \delta U = \delta(um) \tag{6}$$

The variation $\delta E'$ at the initial state refers to the small quantity of mass $\delta m'$, which can be expressed in the general form:

$$\delta E' = e'\delta m' = \left(u' + \frac{1}{2}v^2 + gz + \frac{\mu}{M}\right)\delta m' \tag{7}$$

where specific kinetic and potential energies, as well as the chemical potential normalized by the molar weight M to be consistent with specific energy dimensions, are included. If kinetic, gravitational and chemical effects are neglected as in the final state, it can be deduced:

$$\delta E' = e'\delta m' \simeq u'\delta m' \tag{8}$$

From the previous rationale, Eq. (5) can be written in the form:

$$\delta Q = \delta(um) - u'\delta m' + \delta L_{sys} - p\delta V' \tag{9}$$

where the enthalpy of the mass $\delta m'$ at the initial state can be identified:

$$\delta H' = h'\delta m' = \delta U' + p\delta V' = u'\delta m' + p\delta V' \tag{10}$$

Replacing (10) in (9):

$$\delta Q = \delta(um) - h'\delta m' + \delta L_{sys} \tag{11}$$

Up to this point, if the derivative respect to time is introduced, a differential equation for the transport of heat and energy can be deduced. Assuming that $\delta/\delta t \simeq d/dt$, it can be obtained from (11):

$$\frac{dQ}{dt} = m\frac{du}{dt} + u\frac{dm}{dt} - h'\frac{dm'}{dt} + \frac{dL_{sys}}{dt} \tag{12}$$

Recalling that from the conservation of mass both derivatives of mass equals the mass flow rate, say:

$$\frac{dm}{dt} = \frac{dm'}{dt} = -Q^m \tag{13}$$

Eq. (12) takes a more convenient form for the First Principle for an open system:

$$\boxed{\frac{dQ}{dt} = m\frac{du}{dt} + \left(h' - u\right)Q^m + \frac{dL_{sys}}{dt}} \tag{14}$$

In fact, Eq. (14) is more general than the case of the OWC, since no further restriction has been imposed to L_{sys}. Thinking in terms of an OWC, the work performed on the system by the wave action is a deformation work expressed as:

$$L_{sys} = -\int pdV \tag{15}$$

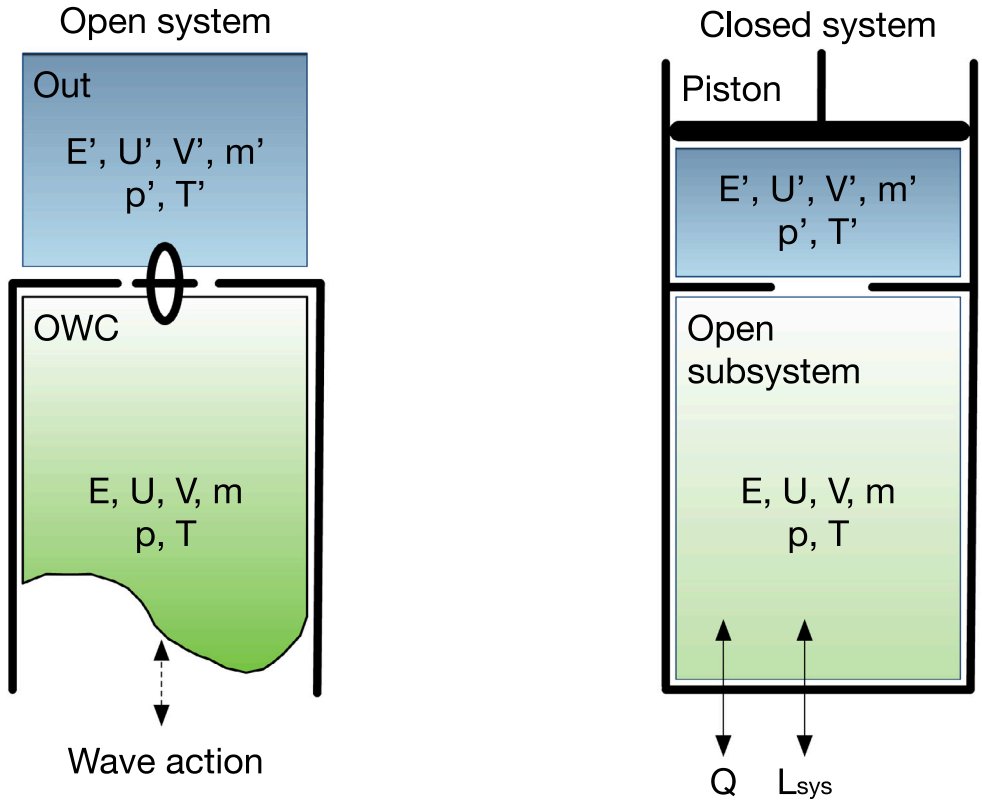

Fig. 1. OWC open system example and closed system model adaption.

with the sign to be fixed upon an arbitrary criterion. If OWC compression is considered and the work performed on the system is considered intrinsically negative, then:

$$L_{sys} \simeq -pV \tag{16}$$

assuming homogeneous pressure inside the OWC. Therefore, assuming that the pressure reaches instantly a state of equilibrium during compression, it is feasible to obtain the equation proposed in Falcão and Justino (1999):

$$\boxed{\frac{dQ}{dt} = m\frac{du}{dt} + \left(h' - u\right) Q_T^m - \left(p_{atm} + p_{owc}\right) Q_{owc}} \tag{17}$$

2.2. Clausius Theorem

According to the Clausius Theorem, a closed system verify:

$$\oint \frac{dQ}{T} \leq 0 \tag{18}$$

where dQ represent the heat exchange during the cyclic process, and T the temperature of the source giving off heat. In the case of a reversible process, the equality is verified, being the inequality satisfied in the case of an irreversible process. Dividing the closed path into two parts, (I) from the point A to the point B, and (II) from the point B to the point A (see Fig. 2), and considering a reversible process, the expression (18) can be rewritten as:

$$S_B - S_A = \int_A^B \frac{dQ}{T} \tag{19}$$

which mean that, in a reversible process, the value of the integral does not depends on the path, so there is a state function S called entropy which only depends on the initial and final states. In the case of a non-reversible process, following the same reasoning:

$$\oint \frac{dQ}{T} = \int_A^B \frac{dQ}{T} + \int_B^A \frac{dQ^{rev}}{T} < 0 \rightarrow S_B - S_A > \int_A^B \frac{dQ}{T} \tag{20}$$

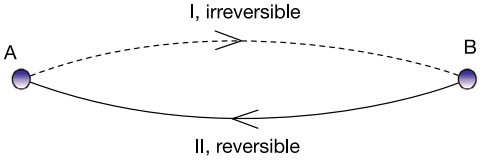

Fig. 2. Cyclical process, Biel (1986).

Joining both results, the Clausius Theorem is obtained:

$$S_B - S_A \geq \int_A^B \frac{dQ}{T} \tag{21}$$

Depending on the value of the integral, or if the equality or inequality is verified, the process is different. The adiabatic process occurs when the value of the integral is 0, and the reversible process occurs when the equality is satisfied. That means that, in an isolated system, the entropy of the system never decrease. But, in the case that the system is not thermally insulated, the entropy can decrease if the system gives heat to the medium, even if it undergoes irreversible processes.

2.3. Thermodynamic process

A general polytropic process of a simple closed system is represented by Eq. (22), Biel (1986):

$$pv_m^n = const \tag{22}$$

where p is the thermodynamic pressure, v_m is the molar volume of the gas, defined as V/N (V is the volume, and N is the number of moles), and n is the polytropic exponent, whose value depends on both the type of process and the nature of the gas ($n = 1.4$ for ideal dry air, $n = 5/3$ for ideal monoatomic gas). Eq. (22) describes the relationship between

thermodynamic variables, as the system evolves through intermediate equilibrium states following a sequence represented by a specific path in the p–V thermodynamic space.

In the case of the compression/expansion cycle during OWC performance, the sequence of (p, V, T) states undergone by the gas inside the chamber, follows the process Eq. (22), the value of polytropic exponent n determined by the nature of the system, either considered as an ideal gas or as a real gas mixture of dry air and water vapour. Therefore, the process equation determines the availability of states as the system evolves under the mechanical work exerted by the water column displacement, i.e. it determines how the system temperature is balanced and heat is exchanged if any. Any combination of (p, V, T) not represented by the process equation is not available for the system, and the deviation is balanced through radiation–diffraction effects.

Following Medina-López et al. (2017b), in the real situation, there is a mixture of dry air and water vapour inside the OWC chamber, so it is necessary to find an explicit form for the polytropic exponent n that describes the real process. For that purpose, applying the compressibility factor Z of the Virial expansion, Prausnitz et al. (1999), the relation between the polytropic index m and polytropic exponent n is:

$$n = Zm \tag{23}$$

where

$$m = \frac{C_y - C_p}{C_y - C_v} \tag{24}$$

where C_p, C_v and C_y represent the specific heats under constant pressure, volume and a certain variable y respectively.

The specific heats C_p and C_v, the molar entropy s, the internal energy u and the enthalpy h for the real gas can be expressed as a variation from the ideal gas as follows:

$$C_p = C_p^* + p\delta C_p = C_p^* - T\frac{d^2B}{dT^2}p \tag{25}$$

$$C_v = C_v^* + \delta C_v = C_v^* - \frac{R_0}{v_m}\frac{d}{dT}\left(T^2\frac{dB}{dT}\right) \tag{26}$$

$$s = s^* + \delta s = s^* - \frac{dB}{dT}p \tag{27}$$

$$u = u^* - T^2\frac{R_0}{v_m}\frac{dB}{dT} \tag{28}$$

$$h = h^* + p\delta h = h^* + Bp - T\frac{dB}{dT}p \tag{29}$$

where "*" represents the ideal gas variables, B is the second virial coefficient, and R_0 is the universal gas constant. To calculate B for any state, it can be used the *Tsonopoulos* expression, Tsonopoulos and Heidman (1990):

$$\frac{Bp_c}{R_0T_c} = f_0 + \omega f_1 + \chi_{mol} f_2 \tag{30}$$

where f_0, f_1 and f_2 are temperature correlation functions, ω is the acentric factor, χ_{mol} is the molar fraction of vapour in dry air, T_c = 647 K and p_c = 218 atm. This method is developed in Medina-López et al. (2017b).

3. Experimental set up

The tests have been carried out in the wave flume of the Hydraulics Laboratory in the School of Civil Engineering of the University of Granada (Spain). The wave flume has the same configuration that the wave flume used in Molina-Salas et al. (2022b). It is a flat-bottomed wave flume, with 10 m long and 1.5 m wide, build inside a wave basin but isolated from the rest of the waterbody by rigid walls, as Fig. 3 shows. At the end of the flume, a dissipative beach is built with the aim to minimize the wave reflection. This dissipative beach is build with concrete cubes of 7.5 cm. Each side, which are on a grid structure that allows the wave to pass through it. The slope of this beach is 2.5 : 1. So, a part of the wave energy is dissipated on the beach, other part is transmitted through it or above it to the rest of the wave basin, and other part is reflected. The paddle system implements a wave absorption system that allows to eliminate the reflected waves. Nevertheless, the focus is placed on the interaction between surface level oscillation inside the chamber and thermodynamic process of the air. The wave propagation along the flume is recorded with four wave gauges located as Fig. 4 shows, one of them placed inside the OWC chamber. The water depth is $h_w = 0.448$ m for all test.

The OWC device model consist into a hollow vertical cylindrical structure 0.60 m high, with an internal diameter D_{OWC} = 0.20 m. The wave energy transmission between the outside and inside of the chamber is allowed by a 0.16 m height gap placed at the base of the cylinder, spanning along its perimeter. Figs. 5 and 6 show respectively the scheme of the geometric configuration of the device, and the device used in the tests. The transition between the diameter of the chamber and that of the turbine has been made with a part with two cone-shaped trunks, as it is shown in Fig. 5. The turbine used is a Wells type turbine, with an external diameter of $D_t = 0.045$ m and an internal diameter of $D_{in} = 0.0225$ m, cross-section area $A_t = 1.39 \cdot 10^{-3}$ m^2 (center to blade tip), 6 divergent blades with an area of $A_b = 1.32 \cdot 10^{-4}$ m^2 each one, solidity of $\sigma = 0.6508$, and NACA0022 profile. The turbine performance is represented by a linear relationship between the pressure drop Δp [Pa] and the rotational speed N [r.p.m.] or the air flow Q [m^3/s]. This OWC device is not scaled from any real OWC device. Indeed, the thermodynamics scale effects essentially become evident when the model is scaled up. So, the scale factor should be applied to extrapolate those results to a full-scaled model, in order to present transient states associated to the homogenization of variables over volumes even larger – see Molina-Salas et al. (2023) –. The turbine size has been fixed to match the chamber size and the wave propagation conditions, i.e. an increase in the size of the turbine might result in a stall effect due to poor wave energy to drive it. Moreover, the objective of this research is to study the air compression/expansion thermodynamic process inside the chamber, rather than its repercussion on the turbine performance, which would be the next step of the research. The turbine is used as a restrain of the system with the aim of reproducing adequately the real performance conditions. Its replacement by a orifice or a porous layer would modify the thermodynamic performance of the system since the pressure–air flow coupling would be modified. In addition, as Authors have indicated in previous research – see Molina-Salas et al. (2023) –, it is very complicated to build an OWC model that satisfies the hydrodynamics, thermodynamics and aerodynamics conditions simultaneously, as well as to build a turbine that respects all the scale relations, like the aerodynamic and inertial forces, the inertia of the rotor, or the mas s of the blades, among others.

Temperature (T), humidity (RH), air velocity (v), static pressure (p) and total pressure (p_{tot}) have been measured both inside and outside the OWC chamber – see Figs. 5 and 6 –. A total of eleven taps have been used to measure static and total pressure. Four taps have been placed inside the chamber – numbers 1 to 4 –, four at the exit of the chamber – numbers 5 to 8 –, and 3 in the outside – numbers 9 to 11 – (numbers 1, 2, 5, 6 and 9 to measuring static pressure; 3, 7 and 10 to measure total pressure pointed downside; and 4, 8 and 11 to measure total pressure pointed upside). All of this gauges are connected to a data acquisition system configured at 50 Hz. The sampling frequency for all the devices have been choose taking into account the Nyquist Theorem. To measure the water elevation, four resistives gauges have been used – three before the OWC, and one inside –, connected to the same system that the rest of the gauges Finally, the rotational speed of the turbine has been measured with a device connected to the same acquisition system.

In Section 4 it will be analysed the thermodynamic process that govern the air response inside the OWC chamber. Although the turbine performance has been measured (the relation between rotational speed of the turbine, pressure drop and air flow through it), its analysis is not the target of this paper.

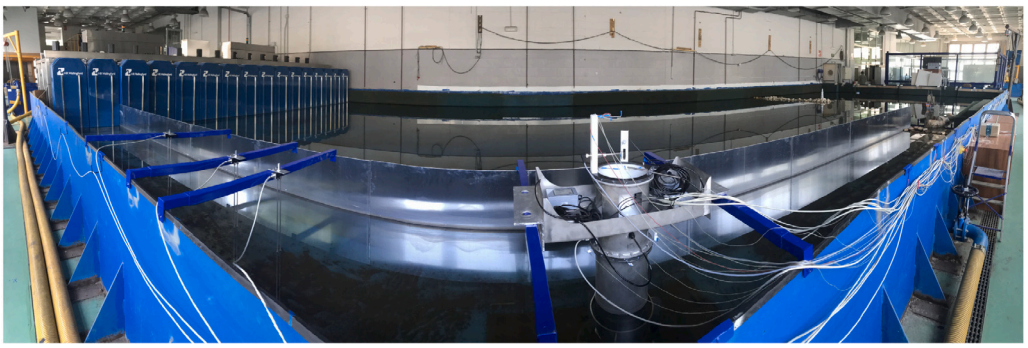

Fig. 3. Wave flume used in this research.

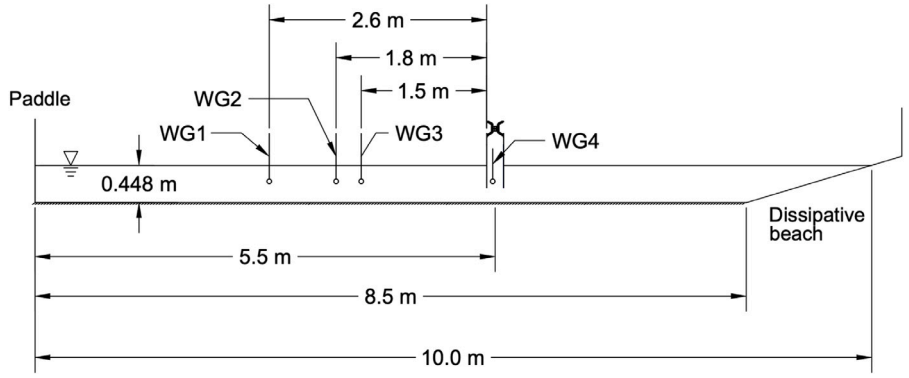

Fig. 4. Wave gauges distribution.

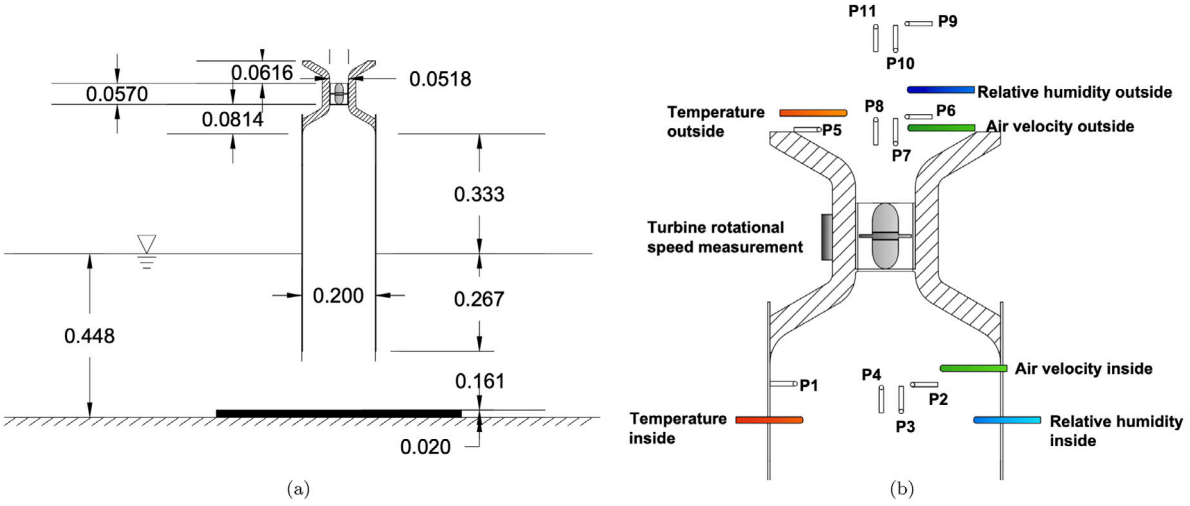

Fig. 5. (a): Geometric configuration of the chamber (dimensions in mm). (b): Pressure taps and gauges distribution.

4. Results and discussion

A total of ten test with regular waves have been conducted. Active wave absorption of the paddles has been enabled. In each one, the relative depth has changed according to Table 1. In this study, the main objective is to estimate the entropy variation and energy budget over the air compression/expansion cycles for a range of wave number values. Results are presented in dimensional form. However generality is preserved since the focus is placed on state functions budget rather than relative magnitude.

The properties of the air are indicated in Table 2.

The methodology used to analyse the thermodynamic processes starts from the pressure time series, which follows a sinusoidal signal. The internal energy, enthalpy and entropy have been calculated in the states of maximum and minimum pressure inside the chamber, distinguishing between expansion (from maximum to minimum pressure states) and compression (from minimum to maximum pressure states). The volume used in those calculations is the value obtained while the maximum and minimum pressures occur. Regarding the temperature, the time series indicates that the temperature is essentially constant during the tests, so the value of temperature used is constant for each test. Following the procedure indicated in Medina-López et al. (2016), the density calculated is constant during all the tests – see Fig. 11 –, which indicates that the air is not compressible during the tests performed. On the other side, to calculate the Clausius Theorem and the work done by/on the system, it has been used the complete

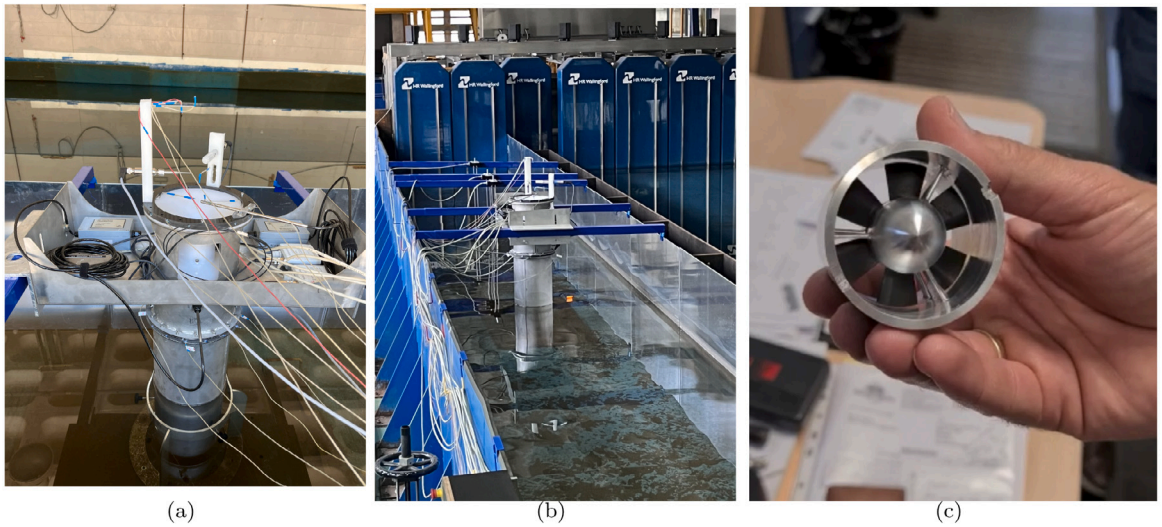

Fig. 6. (a) and (b): OWC device and measure gauges. (c): Wells turbine.

Table 1
Test runs for regular waves (water depth $h_w = 0.448$ m).

Test	Wave height H_s [m]	Wave period T_z [s]	Wave number kh [–]
1	0.10	2.12	0.68
2	0.08	1.01	1.87
3	0.08	1.33	1.21
4	0.08	1.67	0.90
5	0.10	1.67	0.90
6	0.10	2.01	0.72
7	0.10	2.34	0.61
8	0.15	2.01	0.72
9	0.15	2.23	0.61
10	0.15	2.68	0.52

Table 2
Dry air and water vapour properties.

Properties	Value	Units
Air properties		
R_a	286.7	J/kg K
$C_{p,a}$	1010	J/kg K
ρ_a	1.25	kg/m^3
MW_a	0.0288	kg/mole
$T_{c,a}$	132	K
$p_{c,a}$	$3.771 \cdot 10^6$	Pa
Water vapour properties		
R_v	461	J/kg K
$C_{p,v}$	1093	J/kg K
MW_v	0.0182	kg/mole
$T_{c,v}$	647	K
$p_{c,v}$	$2.2089 \cdot 10^7$	Pa

pressure and volume time series in order to estimate the numerical value of the integral that define them. It is clear that, in a strict sense, thermodynamic states refer to equilibrium states. Nevertheless, in practice, it can be considered that the air system follows a sequence of steps between initial and final states, to be considered as fairly in instantaneous equilibrium, so the thermodynamics principles can be applied in such a feasible way.

In this research, no control on turbine-damping have been exerted. However, turbine-damping as a consequence of the coupling between the turbine performance and air chamber compression/expansion is comprehensively considered through the analysis of the pressure–volume relationships governing the processes inside the chamber. This research is focused on the polytropic process curve itself, which in turn implements all damping effects through the state equations, so no restrains on turbine damping other than the natural ones have been considered, in order to observe the compression/expansion process and the heat/entropy budget in the widest range as feasible.

4.1. Energy budget

Energy budget over the air expansion/compression cycles is analysed. Internal energy during the air compression and expansion can be estimated according to Eq. (28), even considering real gas model. The work done by/on the system can be estimated using the measured pressure and the volume of air inside the chamber – calculated through the water surface elevation –. Finally, the heat exchange has not been measured but estimated applying Eq. (17). The results obtained after applying this method to the different cases indicated in Table 1 are shown in Fig. 7.

As seen from Fig. 7 it is important to point out that the internal energy variation of the system over the air expansion/compression cycles is almost null, which means that, according to the first principle of thermodynamics, the process can be considered cyclic. This fact was pointed out by authors in previous researches, Molina-Salas et al. (2022b). Furthermore, during the two phases of the cycle, the internal energy variation is also null, so the same amount of energy rejected or absorbed in form of heat is absorbed or rejected, respectively, in form of work for each phase. Therefore, in order to analyse the energy exchanges in the form of work and heat, a distinction between the air expansion and compression phase is assumed. During the compression phase, the water lever rise drives the system performance and $\Delta l > 0$, i.e. work done on the system. Nevertheless, during this phase, the system is exchanging heat with the environment in order to maintain its internal energy constant, as Fig. 7 shows. During the other part of the cycle, the process is inverted. The air system expands and, in this case, the work is done by the system since $\Delta l < 0$, and the system absorbs some amount of heat, maintaining constant its internal energy. Nevertheless, if more appropriately, the compression phase is interpreted as an *active* process and the expansion interpreted as a vacuum expansion according to the Joule's expansion – *passive* process –, $\Delta l = 0$ during the expansion phase. So, according to the First Principle of thermodynamics, in this case the heat exchange must be null, i.e. the expansion phase is adiabatic. That interpretation is analysed in Section 4.2.

In a more detailed way, Fig. 7 shows that the exchanged heat has not the same value – in absolute terms – that the amount of energy in form of work, neither during the two different phases nor

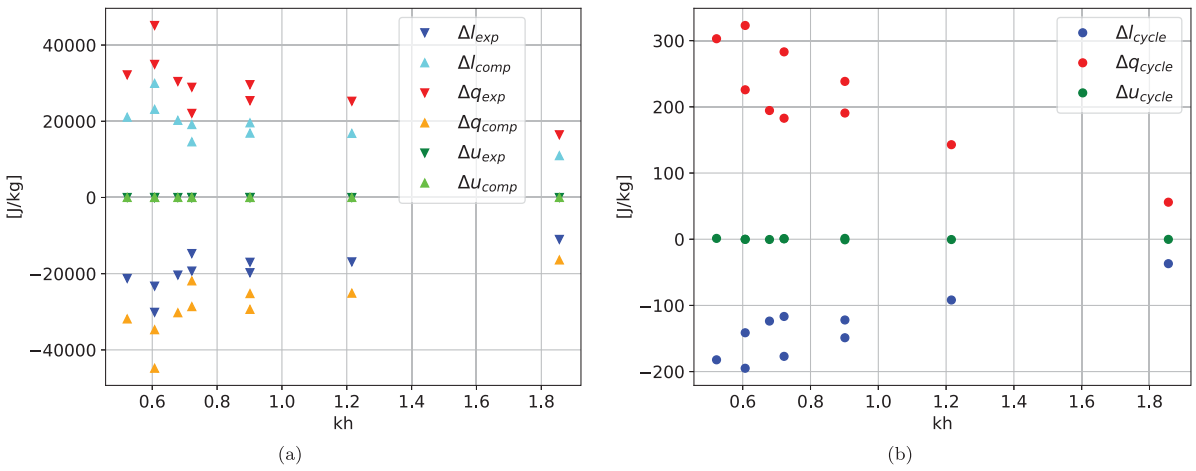

Fig. 7. Internal energy, work and heat exchange during the (a): expansion and compression phases. (b): complete cycle of expansion/compression.

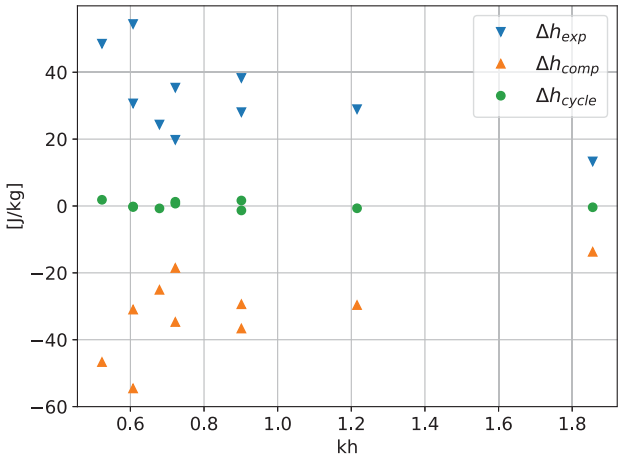

Fig. 8. Enthalpy variation over the expansion/compression cycles.

over the complete cycle. That can be explained with the enthalpy variation shown in Fig. 8 and the indirect way to estimate the heat exchange according to Eq. (17). During the compression phase, some amount of energy is rejected and scattered back to the environment, $\Delta h < 0$, and this amount of energy is introduced in the heat balance according to Eq. (17). During the expansion phase, the process is inverted, and the same amount of energy is now absorbed by the system, $\Delta h > 0$. This amount of energy could be interpreted in different ways: (i) as the kinetic energy of air due to the flow velocity induced by the compression/expansion process through the turbine duct; (ii) as the amount of energy that is transferred between the air and the turbine; or (iii) as the amount of energy that the system exchange with the environment through its boundaries, e.g. the walls of the device. While from Fig. 8 it is not feasible to determine whether the energy (thermo and mechanical) transferred from the system to the turbine is entirely supplied onto the shaft (wall efficiency, as it has been indicated by Dixon and Eng (1966)) or is also exchanged in terms of heat through the boundaries and water surface, it allows to set a maximum range of availability for supplying the turbine rotor from the pneumatic energy resource (isentropic efficiency, Dixon and Eng (1966)).

It is important to point out that, while the Wells turbine is fully represented by a scaled model with solidity $\sigma = 0.6508$ and NACA 0022 blades profile, there is no PTO connection, i.e., no generator is connected to the turbine, hence no utter work is transferred to the shaft. However, from the standpoint of setting up performance limits, the free rotation shaft provides alternatively with a maximum threshold for turbine rotational/flow speed and compression characteristics and performance. The free rotation of the turbine implies a higher rotational speed than a turbine with a brake or connected to a generator system. This fact affects the air compression/expansion process since the pressure reached during the compression phase increase with the rotational speed of the turbine, so the pneumatic power will also increase.

4.2. Thermodynamic process

Once the energy budget of the air expansion/compression cycle has been explained, it follows an interpretation of the different phases. Fig. 9 is used as a reference for this interpretation. As it has been indicated in Section 4.1, the compression phase is an *active* process where the work is done on the system —$\Delta l > 0$— and the system rejects some amount of heat —$\Delta q < 0$—. In this phase, the system works on the turbine and the external ambient manostat, yielding energy (kinetic and/or thermal) to them since $\Delta h < 0$. This process can be assimilated to a conversor of work into heat, as it is defined by Biel (1986). According to this thermodynamic machine scheme, all the energy in form of work done on the system is transformed into heat, so the internal energy balance is null, like it is depicted Fig. 7. In addition, during this phase the entropy decreases, $\Delta s < 0$ due to that amount of heat rejected, as Fig. 10(a) shows. Nevertheless, during this phase, the Clausius Theorem is verified – see Fig. 10(b) –, so the process is realizable even entropy is decreasing.

During the other part of the cycle, usually named *expansion*, the method described in Section 4.1 to estimate the heat exchange indicates that the system absorbs heat from the environment. So, in this case the Clausius Theorem is not satisfied since $\Delta s < \int dq/T$ as Fig. 10 shows. Nevertheless, as it is indicated in Section 4.1, the method used to estimate the energy balance in this phase may not be appropriate. Although the work done by the system during this phase can be calculated using the pressure–volume states measured, its negative value can be interpreted as the water level decreases due to the work done by the system over the boundaries of the device. Nevertheless, the water level decreases because its natural movement. For that reason, that phase can be interpreted in a more appropriately way as Joule expansion. According to this interpretation, when the water level decreases a momentary vacuum space is created, which causes that the pressure decreases and the air can expands freely without exerting any work. Applying the First Principle of thermodynamics, the heat exchange during this phase would be also null since $\Delta u = \Delta l = 0$. In addiction, the Joule expansion also establish that the entropy increases during the free expansion, as the experimental data shows. Therefore, the Clausius Theorem would be totally satisfied since $\Delta s > \int dq/T = 0$, and the process is realizable. Finally, the enthalpy increase during this phase

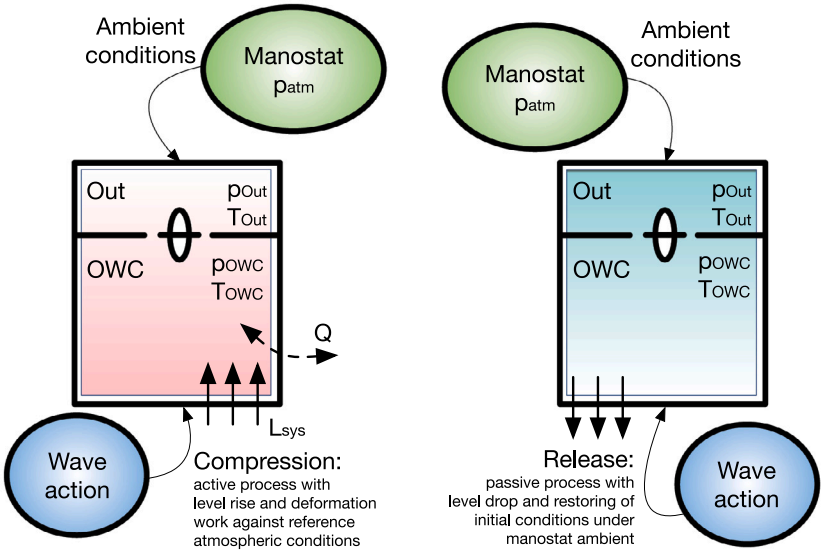

Fig. 9. Scheme of the different phases performance of the OWC device.

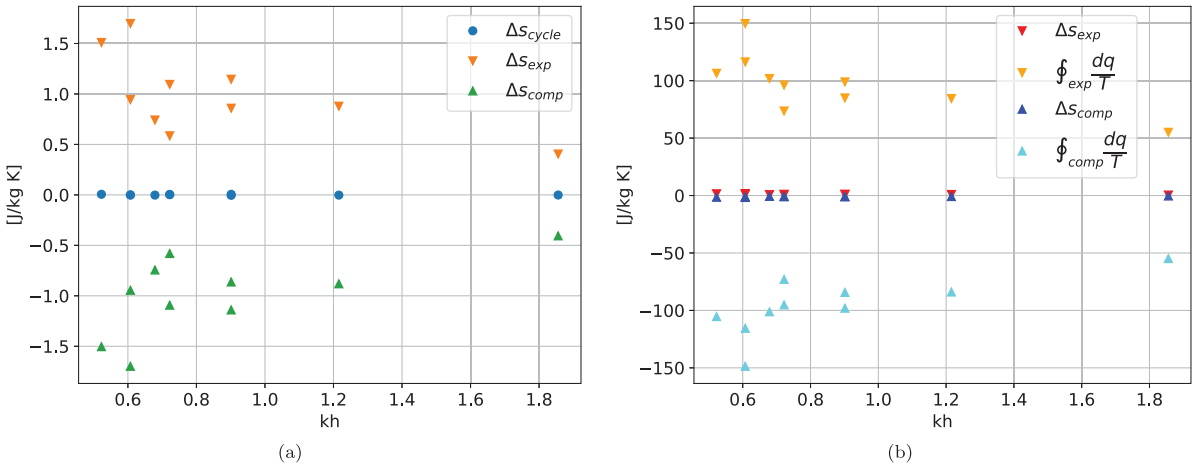

Fig. 10. (a): Entropy variation over the cycles and semicycles of expansion/compression. (b): Clausius Theorem applied to the air compression/expansion cycles.

can be explained as the energy transmitted from the manostat or the turbine – the environment – to the system.

Therefore, according to that reasoning, rather than compression and expansion cycles, the air process could be more precisely described as a compression (active) process driven by the incident wave action and the water level rise inside the chamber, and a release (passive) process restoring the initial compression conditions, and driven by: (1) the back scattering wave action and the lowering of surface level inside the chamber, and (2) the outer conditions governed by the monastic boundary conditions represented by the atmospheric pressure.

All in all, the OWC auxiliar system performance through wave cycles can be quantitatively interpreted as a compression subcycle in which the air subsystem inside the chamber "actively" perform on the turbine transforming pneumatic/thermal energy to the rotor (isentropic efficiency), and an expansion cycle during which the air subsystem inside the chamber "passively" expands as a consequence of downward water surface motion, allowing the turbine to be driven by the inverted pressure conditions between the inside (expansion vacuum) and the outside (surrounding atmosphere monastic conditions).

This scheme is compared with the fact that the work transferred to the turbine by the driving subsystem during the compression/release cycle via the pressure variation is not depending on the flow direction, but rather on the velocity magnitude somehow. Hence, pressure drives the flow direction determining which subsystem compresses the turbine (work transferred to the turbine $\rightarrow \Delta h < 0$) and the energy budget (mechanical and thermal) is set by temperature and velocity values. For each cycle, there is one subsystem acting as a "driving" and another acting as "passive" following the scheme in Fig. 9.

It is important to highlight that the temperature is essentially constant during the tests performed, as Fig. 11(a) shows. This figure represents the temperature, pressure, humidity and density evolution during the test number 7 indicated in Table 1, but the results are equivalent for the rest of the tests indicated in this table. This non variation of the temperature during the test indicates that the air compression/expansion process is isotherm, which means that some amount of heat is exchanged between the air system and the environment to keep the temperature constant over the cycles. So, by definition, the process cannot be adiabatic. On the other hand, the analysis of the polytropic exponent points out in the same direction, as it is shown in Fig. 11(b). The value of the polytropic exponent calculated for the tests is $n \approx 1$, which indicates that the process is isotherm – by definition, the value of the polytropic exponent for an isotherm process is $n = 1$ –. In addition, shall the process be adiabatic, the heat exchange and the entropy variation should be null. However that is not the case since the entropy variation over the air expansion/compression process is not null.

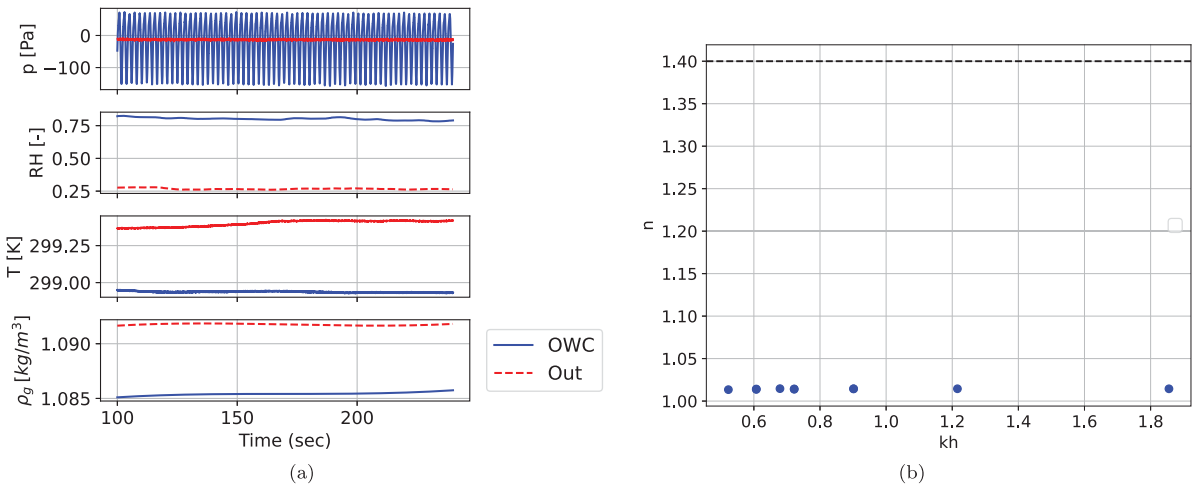

Fig. 11. (a) Pressure, relative humidity, temperature and air density evolution during the test number 7 indicated in Table 1, both inside and outside the OWC chamber. (b) Polytropic exponent obtained for the different cases indicates in Table 1.

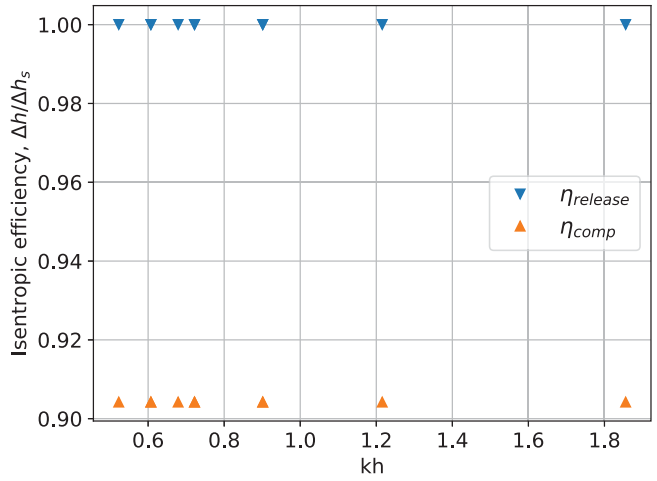

Fig. 12. Isentropic efficiency for the cases indicated in Table 1.

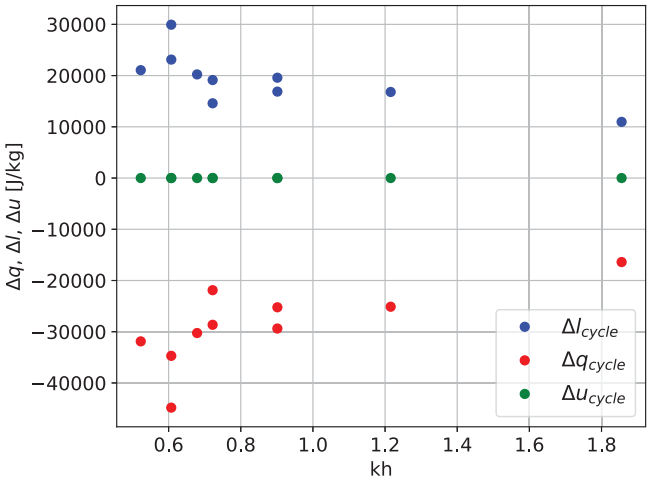

Fig. 13. Energy budget over the complete cycles taking into account an *active* compression and a *passive* expansion.

To finish the analysis of the thermodynamic process, the isentropic efficiency defined by Dixon and Eng (1966) is going to be used. This efficiency, defined as $\eta = \Delta h/\Delta h_s$, where Δh is the enthalpy variation between both sides of the turbine, and Δh_s is the enthalpy variation in the ideal case, i.e., the isentropic process. This definition of efficiency indicates if the real process is closer or further away from the ideal process where the entropy variation is null, i.e., the adiabatic process. Therefore, taking into account the heat exchanged during the two phases of the complete cycle of compression/release, the isentropic efficiency has been estimated. During the restore of the initial conditions phase, the heat exchanged by the system is null, so the isentropic efficiency es 100% due to this adiabaticity. Nevertheless, during the compression phase, the heat exchanged is not null, so this phase cannot be considered adiabatic. This heat exchange makes the process move away from the adiabatic process, so the isentropic efficiency in this phase is reduced to 90.42%. This results are shown in Fig. 12.

Finally, it is important to point that the goal of the research is to get a comprehensive sight of the phenomena involved in compression/expansion processes, as a way to assess efficiency in terms of wave characteristics (wave number). As part of the future research, the first step is to conduct tests under irregular waves to check the performance of the OWC. From that on, simulation of wave climate will provide confidence intervals of performance, efficiency and renewability.

4.3. Repercussion on the LCOE and carbon footprint

Finally, the implications of the energy budget into the cost of the energy produced with this technology are analysed. During a complete cycle, the heat exchange budged is negative —$\Delta q_{comp} < 0$ and $\Delta q_{exp} = 0$—, and the energy budged in the form of work is positive —$\Delta l_{comp} > 0$ and $\Delta l_{exp} = 0$—, as Fig. 13 shows. That means that during a cycle, the system increases its internal energy in the form or work and rejects some amount of heat. The differences between the heat rejected and the work done on the system – in absolute terms – is the amount of energy transmitted to the turbine – useful energy – and the energy exchanged with the environment – wasted energy –. In a more detailed way, focusing on Fig. 13, it can be observed that in a complete cycle of compression/release, the relation $\Delta l/\Delta q \approx 66.69\%$, which means that, during the complete cycle, 33.31% of the work done by the system is transmitted to the turbine, and exchanged with the medium. Applying the exergy efficiency definition – according to *Eq. (25)* in Molina-Salas et al. (2022b) –, the useful energy, i.e. the energy transmitted to the turbine, can be estimated as $(1 - \Delta l/\Delta q) \cdot \eta_{ex}$. The exergy efficiency variation vs. the relative depth is shown in Fig. 14 and the useful energy – expressed as a percentage of the total energy transmitted to the system – is shown in Table 3.

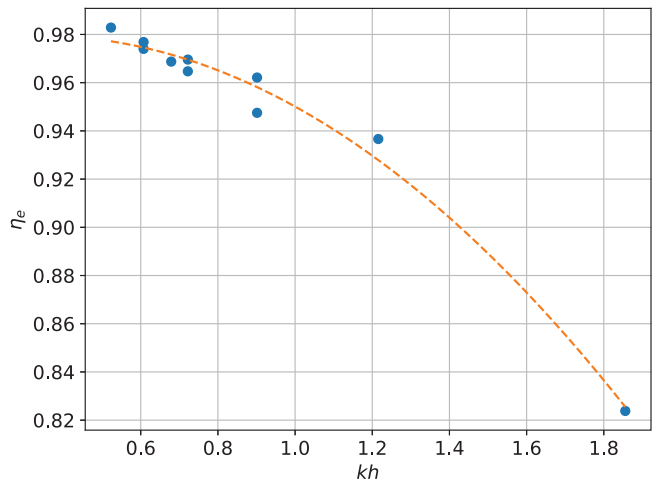

Fig. 14. Exergy efficiency for the cases indicated in Table 1.

Table 3
Exergy efficiency and LCOE repercussion.

Test	Wave number	Exergy efficiency	Useful energy	LCOE
1	0.68	96.87 %	32.27 %	464.85 £
2	1.87	82.38 %	27.44 %	546.63 £
3	1.21	93.66 %	31.20 %	480.79 £
4	0.90	94.75 %	31.56 %	475.27 £
5	0.90	96.21 %	32.05 %	468.04 £
6	0.72	96.47 %	32.13 %	466.79 £
7	0.61	97.40 %	32.44 %	462.33 £
8	0.72	96.96 %	32.30 %	464.45 £
9	0.61	97.68 %	32.54 %	460.99 £
10	0.52	98.29 %	32.74 %	458.17 £

The power obtained with this OWC model can be extrapolated to a full-scaled OWC device. Let suppose a real OWC with 2 meters of diameter, which would mean a scale factor of $\lambda = 0.1$ respect the OWC device performed during the tests. According to Froude similarity, the ratio between the power output of the prototype and the model is $r_W = \lambda^{7/2}$. Now, let consider an OWC device placed in the Mediterranean Sea where, according to Medina-López et al. (2019), the statistical analysis indicates that, in one year, there would be 3000 waves with a period of 7 s and 100 waves with a period of 10 s. So, extrapolating the data obtained for the present research, the power output obtained in this situation would be fairly around 4 MWh/year with a single OWC device, which is a reasonable value considering the small size of the scaled up turbine. This value indicates that the results of the tests performed are reasonable.

The useful energy can be interpreted as a factor that has a direct influence on the Levelized Cost of Energy ($LCOE$). According to de Andres et al. (2017), the LCOE is defined as:

$$LCOE = \frac{NPV(CAPEX + OPEX)}{AEP} \tag{31}$$

where NPV is the net present value, calculated following Têtu and Fernandez-Chozas (2021) as:

$$NPV = \frac{i}{1-(1+i)^{-(n+1)}} \tag{32}$$

where i is the interest rate and n is the life time. According to de Andres et al. (2017), $i = 12\%$ and $n = 25\ years$. The CAPEX and OPEX values are necessary to estimate the LCOE of the OWC device. The analysis of the LCOE in this research starts from the results obtained by de Andres et al. (2017), where the CAPEX, OPEX, AEP and LCOE has been estimated. From that on, in the present rationale, it has been assumed that the energy budget essentially affects only the energy production (the AEP value), so taking the same values of capital and operative expenses (CAPEX and OPEX) than the mentioned research as a reference, the value of the AEP due to the energy budget obtained has been estimated, and a new value of LCOE has been calculated.

The useful energy expressed in Table 3 can be interpreted as a corrective factor of AEP, i.e. as a factor to reduce the annual electricity production as $AEP_{corr} = AEP \cdot \%Useful\ energy$. In this case, applying the same values of NPV, $CAPEX$ and $OPEX$ as de Andres et al. (2017), and applying the explained correction for the values of AEP obtained by de Andres et al. (2017), the $LCOE$ values increase from 150 £/MWh – $LCOE$ target establish in de Andres et al. (2017) – to the values shown in Table 3. This means that the $LCOE$ increases between the 305% and 364%.

From another point of view, those results can be used not only as a factor to modify the $LCOE$, but as a factor to limit the maximum amount of energy that could be produced. This limit in the maximum amount of energy that a plant can reach can be used to improve the design of this plants with the aim of reducing the $CAPEX$. This is consistent with previous researches – Jalón et al. (2016) –, where it was pointed out that the efficiency – understood as the LCOE – of the OWC device improves when this devices are designed to average climate conditions.

In a step further, some considerations imported from emergy analysis bring to front that OWC technology can provide with a even more efficient performance. An emergy-based analysis of renewability – and of sustainability in a wider socio-economic sense – of the proposed performance of an OWC model, would require not only technical data during the operating phase, but also tracked information on natural resources, renewable and non-renewable inputs as well as human and economic resources flux from the society – see for example Yang and Chen (2016), Brown and Ulgiati (2002) –. In that sense, exergy analysis provides with a strictly thermodynamic and efficiency focusing. Even if exergy and emergy analysis can be related accurately – Bastianoni et al. (2016) –, there are required variables that might not be available in all cases. Nonetheless, from the definition of some emergy-based descriptors and starting from the information provided by the exergy analysis, it is feasible to define some descriptors that can utterly be used to relate exergy renewability with emergy descriptors and with greenhouse emissions, which is a key factor when relating renewability – a pure thermodynamic concept, Molina-Salas et al. (2022b) –, with impacts on the biosphere. In that sense, a *renewable emergy index* can be defined as:

$$\lambda_{em} = EIS \cdot \frac{F}{R} = \frac{Y}{N+F} \tag{33}$$

where *EIS* is the emergy index of sustainability – (Brown and Ulgiati, 2002) –, Y is the total emergy assigned to the output, calculated as the sum of the renewable (R), non–renewable (N) and purchased feedback flows of goods and human services from the economy (F). This λ_{em} can be considered as the equivalent to the renewability index defined in terms of exergy balance – de Oliveira (2013) –:

$$\lambda_{ex} = \frac{\sum e_{out}}{e_{nr} + e_{dt} + e_{da} + e_{da} + \sum e_{em}} \tag{34}$$

Given the relation between emergy and exergy, descriptors can be drawn in terms of transformation factors. It can be expected that in any given non-dimensional combination, the magnitude of relations be preserved. For that reason, it is expected that in non-dimensional terms, the definitions of λ_{em} and λ_{ex} represent the same magnitude, say, the balance between the power output and the non-renewable sources and derived process, hence $\lambda_{em} \sim \lambda_{ex}$.

From that previous statement, it can be estimated the balance between avoided and released GHG emissions in OWC operating in the same fashion as it can be conducted for other types of renewable power plants. Let us consider first the balance of $CO_{2,avoided}/CO_{2,released}$ corresponding to wind, geothermal and hydroelectric plants according to *Table 3* in Brown and Ulgiati (2002). Those values have been obtained from ENEA (1996). Although those values should be updated,

Table 4
Comparison of energy indicators and GHG flows for different electricity production systems.

	Wind (2.5 MW)	Geothermal (20 MW)	Hydro (85 MW)	OWC (0.005 MW)
Total electric energy produced per year [J]	$1.35 \cdot 10^{12}$	$3.28 \cdot 10^{14}$	$3.94 \cdot 10^{14}$	$1.06 \cdot 10^{9}$
CO_2 released [g]	$1.36 \cdot 10^{7}$	$5.98 \cdot 10^{10}$	$1.27 \cdot 10^{9}$	$3.03 \cdot 10^{3}$
CO_2 avoided [g]	$3.39 \cdot 10^{8}$	$8.25 \cdot 10^{10}$	$9.91 \cdot 10^{10}$	$2.67 \cdot 10^{5}$
CO_2 ratio (avoided/released)	25.02	1.38	77.752	87.82
Renewability emergy index, λ_{em}	7.44	3.30	3.21	30

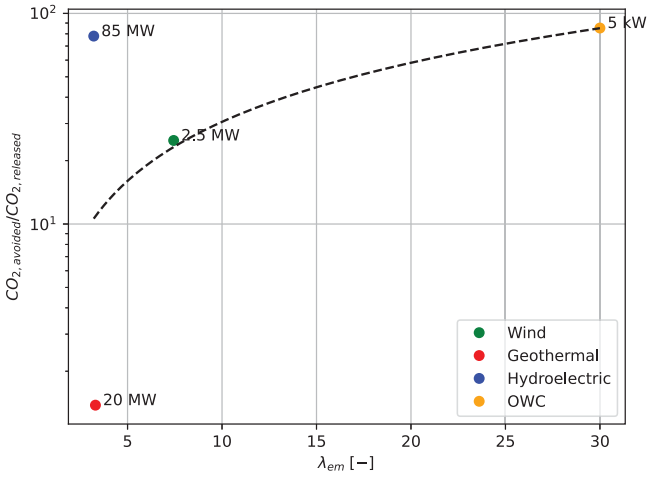

Fig. 15. Ratio $CO_{2,avoided}/CO_{2,released}$ vs. renewability emergy index for different electricity production plants.

they give us a first approach to compare the emergy analysis of the OWC device with the rest of renewable electricity production systems. From that information and using the definitions in Eq. (33), the relation between $CO_{2,avoided}/CO_{2,released}$ in plant operating is represented in Fig. 15. This figure represents a tendency fit for the three renewable power plants indicated in the mentioned *Table 3* in Brown and Ulgiati (2002). The ratio of $CO_{2,avoided}/CO_{2,released}$ for the OWC power plant has been estimated using the mentioned adjustment and applying a value of $\lambda_{ex} \sim \lambda_{em} = 30$, according to Molina-Salas et al. (2022b).

Now, let us considerer a simple OWC device with a generating capacity of 5 kW, and let us assume that $\lambda_{em} \equiv \lambda_{ex}$. If the device is installed on location where the relative depth is $kh \approx 0.68$, the capture length would be $kL \approx 0.031$ and the renewability index is $\lambda_{ex} \sim \lambda_{em} \approx 30$. So, according to the data represented in Fig. 15, the relation between $CO_{2,avoided}/CO_{2,released}$ for the OWC device can be estimated in 87.82. Considering a capacity factor of 0.28 – similar to the data available from Mutriku Power Plant –, and a turbine efficiency of $\eta_{turb} = 75\%$, the annual electric energy produced by the device is $1.06 \cdot 10^9$ J. If this amount of electricity would be generated by conventional fossil fuel systems (a thermal plant), the amount of CO_2 released to the atmosphere, and thus, avoided by the OWC device, is $2.67 \cdot 10^5$ $g\,CO_2$/year, which means that the amount of GHG emissions is $3.03 \cdot 10^3 g\,CO_2$/year during its lifetime. Table 4 shows the comparison of this example with other production systems – (Brown and Ulgiati, 2002) –.

As it can be seen in Table 4, although the amount of energy that the OWC system can produce nowadays is lower than other renewable sources, the value of CO_2 ratio is at least in the same range than other renewable systems, or even higher. Focusing in the renewability emergy index, the value is also in the same range or higher, depending on the wave conditions according to Molina-Salas et al. (2022b). That means that the OWC system can be an alternative to the conventional fuel systems and will help to reduce the GHG emitted.

5. Conclusions and future research

In this research, an energy budget of an OWC device performance has been conducted from experimental data, with the aim to set a maximum efficiency of the device and to obtain a factor to correct the cost of it. In addition, an estimation of the carbon footprint of these devices has been studied. The main conclusion of this research are:

- The process can be considered as cyclic given $\Delta U_{cycle} = 0$. On the other hand, the null entropy variation over a complete cycle points out to the same concept. That means that the air system can be considered in fact as an auxiliar system and the OWC device can be considered as a thermodynamic machine, according to the scheme proposed in Molina-Salas et al. (2022b).
- Despite this cyclical behaviour, the different phases of each cycle present different behaviour. One phase is an *active* phase of compression, where the work is done on the system and the system reject some amount of heat to the environment. The other part of the cycle is a *passive* release process where the initial conditions are restored. In this phase, a free expansion takes place, in which the work done by/on the system and the heat exchange are null.
- The difference between the work done by/on the system and the heat exchanged over the cycles is 33.31%, and can be explained through the enthalpy variation. The enthalpy variation over the expansion and compression phases explains this energy exchange between the system and the environment. The 27.44%–32.74% of this energy is transmitted to the turbine (useful energy) and the rest is transmitted to the environment (wasted energy).
- Although the restoring of the initial conditions phase is an adiabatic process, the compression phase is not adiabatic, differing in this case from the ideal conditions. That heat exchange reduces the efficiency of the device to 90.42%, which implies that the LCOE increases between 205.45% and 264.42%. Consequently, an alternative to reduce the cost of the energy can be to design the device for mild climatic conditions in order to reduce the CAPEX and, consequently, the LCOE.
- The estimative emergy analysis reveals that the OWC system values of avoided/released CO_2 ratio and renewability emergy index are in the same range that other renewable energy systems, which means that this technology can be a real alternative to reduce the GHG emissions and the impacts on the biosphere.

Next steps spinning from this research are: (i) To isolate the external subsystem. This isolation will allow to check if the efficiency of the OWC device could increase. (ii) To test different types of turbines in order to check the influence of this restraint to the system. (iii) To test this device under irregular waves, trying to reproduce real situations and to estimate the efficiency of this device in a more realistic way. (iv) To make a deeper research on the emergy analysis of the OWC device.

CRediT authorship contribution statement

A. Molina-Salas: Conceptualization, Formal analysis, Investigation, Methodology, Writing – original draft, Writing – review & editing, Data curation. **Rami Hatafi:** Data curation, Investigation. **F. Huertas-Fernández:** Conceptualization, Writing – review & editing. **M. Clavero:**

Project administration, Supervision, Writing – review & editing, Resources. **A. Moñino:** Conceptualization, Project administration, Resources, Supervision, Writing – original draft, Writing – review & editing.

Declaration of competing interest

The authors declare that they have no known competing financial interests or personal relationships that could have appeared to influence the work reported in this paper.

Data availability

Data will be made available on request.

Acknowledgements

This work was funded by grant TED2021-131717B-I00 fundec by MCIN/AEI/10.13039/501100011033 and, as appropriate, by ERDF A way of making Europe, by the European Union and by the European Union NextGenerationEU/PRTR, as continuation of the projects P18-RT-3595 and B-RNM-346-UGR18 funded by Andalusian Regional Government.

References

Abanades, J., Greaves, D., Iglesias, G., 2014a. Coastal defence through wave farms. Coast. Eng. 91, 299–307.
Abanades, J., Greaves, D., Iglesias, G., 2014b. Coastal defence using wave farms: The role of farm-to-coast distance. Renew. Energy 75, 572–582.
Abanades, J., Greaves, D., Iglesias, G., 2014c. Wave farm impact on the beach profile: a case study. Coast. Eng. 86, 36–44.
Bastianoni, S., Facchini, A., Susani, L., Tiezzi, E., 2016. Emergy as a function of exergy. Energy 32, 1158–1162.
Bergillos, R.J., López-Ruiz, A., Medina-Lopez, E., Moñino, A., Ortega-Sánchez, M., 2018. The role of wave energy converter farms on coastal protection in eroding deltas, Guadalfeo, Southern Spain. J. Clean. Prod. 171, 356–367.
Biel, Gayé J., 1986. Formalismo y método de la termodinámica. In: Teoría General, Aplicaicones Y Ejercicios Resueltos. Apuntes de clase. Universidad de Granada, p. 258.
Boccotti, P., Filianoti, P., Fiamma, V., Arena, F., 2007. Caisson breakwaters embodying an OWC with a small opening—Part II: A small–scale field experiment. Ocean Eng. 34, 820–841.
Brown, M.T., Ulgiati, S., 2002. Emergy evaluations and environmental loading of electricity production systems. J. Clean. Prod. 10, 321–334.
Cruz, J., 2008. Ocean Wave Energy. Current Status and Future Perspectives. Springer–Verlag, ISBN: 978-3-540-74894-6, p. 431.
de Andres, A., Medina-Lopez, E., Crooks, D., Roberts, O., Jeffrey, H., 2017. On the reversed LCOE calculation: design constraints for wave energy commercialization. Int. J. Mar. Energy 18 (2017), 88–108.
de Oliveira, Jr., S., 2013. Exergy. Production, Cost and Renewability. Springer, ISBN: 978-1-4471-4164-8, p. 336.
Dimakopoulos, A., Cooker, M.J., Bruce, T., 2017. The influence of scale on the air flow and pressure in the modelling of oscillating water column wave energy converters. Int. J. Mar. Energy 19, 272–291.
Dixon, S.L., Eng, B., 1966. Fluid mechanics. In: Thermodynamics of Turbomachinery, fourth ed. Butterworth–Heinemann, ISBN: 0-7506-7059-2.
ENEA, 1996. Final Report of the Research Project on Sustainability of Electricity Production. Research Contract ENEA – University of Siena, Italy, Updated, 2000.
Evans, D.V., 1982. Wave power absorption by systems of oscillating pressure distributions. J. Fluid Mech. 114, 481–499.
Evans, D.V., Porter, R., 1995. Hydrodynamic characteristics of an oscillating water column device. Appl. Ocean Res. 17, 155–164.
Falcão, A.F. de O., 2010. Wave energy utilization: A review of the technologies. Renew. Sustain. Energy Rev. 14 (3), 899–918.
Falcão, A.F. de O., Henriques, J.C.C., 2014. Model–prototype similarity of oscillating–water–column wave energy converters. Int. J. Mar. Energy 6, 18–34.
Falcão, A.F. de O., Henriques, J.C.C., 2016. Oscillating water column wave energy converters and air turbines: A review. Renew. Energy 85, 1391–1424.
Falcão, A.F. de O., Henriques, J.C.C., 2019. The spring–like air compressibility effect in oscillating water column wave energy converters: Review and analyses. Renew. Sustain. Energy Rev. 112, 483–498.
Falcão, A.F. de O., Henriques, J.C.C., Gomes, R.P.F., Portillo, J.C.C., 2022. Theoretically based correction to model tests results of OWC wave energy converters to account for air compressibility effect. Renew. Energy 198, 41–50.
Falcão, A.F. de O., Justino, P.A.P., 1999. OWC wave energy devices with air flow control. Ocean Eng. 26, 1275–1295.
Falcão, A.F. de O., Sarmento, A.J.N.A., Gato, L.M.C., Brito-Melo, A., 2020. The pico OWC wave power plant: Its lifetime from conception to closure 1986—2018. Appl. Ocean Res. 98, 102104.
Fenu, B., Bonfanti, M., Bardazzi, A., Pilloton, C., Lucarelli, Mattiazzo, G., 2023. Experimental investigation of a Multi–OWC wind turbine floating platform. Ocean Eng. 281, 114619.
Fox, B.N., Gomes, R.P.F., Gato, L.M.C., 2021. Analysis of oscillating–water–column wave energy converter configurations for integration into caisson breakwaters. Appl. Energy 295, 117023.
Gabriel Ibarra-Berastegi, G., Sáenz, J., Ulaziad, A., Serras, P., Esnaola, G., Garcia-Soto, C., 2018. Electricity production, capacity factor, and plant efficiency index at the mutriku wave farm (2014—2016). Ocean Eng. 147, 20–29.
Gato, L.M.C., Henriques, J.C.C., Carrelhas, A.A.D., 2022. Sea trial resutls of the biradial and wells turbines at mutriku wave power plant. Energy Convers. Manage. 268, 115936.
Gonçalves, J.D., Teixeira, P., 2022. The effect of the environment humidity on the performance of an oscillating water column wave energy converter. J. Braz. Soc. Mech. Sci. Eng. 44, 46. http://dx.doi.org/10.1007/s40430-021-03348-z.
Huertas-Fernández, F., Clavero, M., Reyes-Merlo, M.A., Moñino, A., 2021. Combined oscillating water column & hydrogen electrolysis for wave energy extraction and management. a case study: The Port of Motril (Spain). J. Clean. Prod. 324, 129143.
Jalón, L., María, L., Baquerizo, A., Losada, M.A., 2016. Optimization at different time scales for the design and management of an oscillating water column system. Energy 95, 110–123.
Josset, C., Clément, A.H., 2007. A time–domain numerical simulator for oscillating water column wave power plants. Renew. Energy 32, 1379–1402.
Kestin, J., 1966. A Course in Thermodynamics. Vol. 1. Blaisdell Publishing Company, p. 615, Library of Congress Catalog Card Number 66 – 10104.
López, I., Carballo, R., Taveira-Pinto, F., Iglesias, G., 2020. Sensitivity of OWC performance to air compressibility. Renew. Energy 145, 1334–1347.
Magagna, D., Uihlein, A., 2015. Ocean energy development in Europe: Current status and future perspectives. Int. J. Mar. Energy 11, 84–104.
Martins-Rivas, H., Mei, C.C., 2009. Wave power extraction from an oscillating water column at the tip of a breakwater. J. Fluid Mech. 626, 395–414.
Medina-López, E., Bergillos, R.J., Moñino, A., Clavero, M., Ortega-Sánchez, M., 2017a. Effects of seabed morphology on oscillating water column wave energy convertersn. Energy 135, 659–673.
Medina-López, E., Borthwick, A., Moñino, A., 2019. Analytical and numerical simulations of an oscillating water column with humidity in the air chamber. J. Clean. Prod. 238, 117898.
Medina-López, E., Moñino, A., Borthwick, A.G.L., Clavero, M., 2017b. Thermodynamics of an OWC containing real gas. Energy 135, 709–717.
Medina-López, E., Moñino, A., Clavero, M., Del Pino, C., Losada, M.A., 2016. Note on a real gas model for OWC performance. Renew. Energy 85, 588–597.
Mendoza, E., Dias, J., Didier, E., Fortes, C.J.E.M., Neves, M.G., Reis, M.T., Conde, J.M.P., Poseiro, P., Teixeira, P.R.F., 2017. An integrated tool for modelling oscillating water column (OWC) wave energy converters (WEC) in vertical breakwaters. J. Hydro-Environ. Res. http://dx.doi.org/10.1016/j.jher.2017.10.007.
Mendoza, E., Silva, R., Zanuttigh, B., Angelelli, E., Andersen, T., Martinelli, L., Nørgaard, J., Ruol, P., 2014. Beach response to wave energy converter farms acting as coastal defence. Coast. Eng. 87, 97–111.
Molina-Salas, A., Jiménez-Portaz, M., Clavero, M., Moñino, A., 2022a. The effect of turbine characteristics on the thermodynamics and compression process of a simple OWC device. Renew. Energy http://dx.doi.org/10.1016/j.renene.2022.03.106.
Molina-Salas, A., Longo, S., Clavero, M., Moñino, A., 2023. Theoretical approach to the scale effects of an OWC device. Renew. Energy 219, 119579.
Molina-Salas, A., Quirós, C., Gigant, P., Huertas-Fernández, F., Clavero, M., Moñino, A., 2022b. Exergy assessment and sustainability of a simple off–shore oscillating water column device. Energy 264.
Moñino, A., Quirós, C., Mengíbar, F., Medina-López, E., Clavero, M., 2020. Thermodynamics of the OWC chamber: Experimental turbine performance under stationary flow. Renew. Energy 155, 317–329.
Morais, F.J.F., Carrelhas, A.A.D., Gato, L.M.C., 2023. Biplane–rotor Wells turbine: The influence of solidity, presence of guide vanes and comparison with other configurations. Energy 262768, 127514.
O'Hagan, A.M., Huertas, C., O'Callaghan, J., Greaves, D., 2016. Wave energy in Europe: Views on experiences and progress to date. Int. J. Mar. Energy 14, 180–197.
Portillo, J.C.C., Gato, L.M.C., Henriques, J.C.C., Falcão, A.F.O., 2023. Implications of spring-like air compressibility effects in floating coaxial–duct OWCs: Experimental and numerical investigation. Renew. Energy 212, 478–491.
Prausnitz, J., Lichtenthaler, R., Gomes de Azevedo, E., 1999. Molecular Thermodynamics of Fluid–Phase Equilibria. Prentice–Hall, ISBN: 0-13-977745-8, p. 864.
Sarmento, A.J.N.A., Falcão, A.F. de O., 1985. Wave generation by an oscillating surface–pressure and its application in wave–energy extraction. J. Fluid Mech. 150, 467–485.
Sarmento, A.J.N.A., Gato, L.M.C., Falcão, A.F. de O., 1990. Turbine–controlled wave energy absorption by oscillating water column devices. Ocean Eng. 17 (5), 481–497.

Setoguchi, T., Takao, M., Santhakumar, S., Kaneko, K., 2004. Study of an impulse turbine for wave power conversion: Effects of Reynolds number and hub–to–tip ratio on performance. J. Offshore Mech. Arct. Eng. 126 (2), 137–140.

Sheng, W., Alcorn, R., Lewis, S., 2013. On thermodynamics of primary energy conversion of OWC wave energy converters. J. Renew. Sustain. Energy 5, 023105.

Sheng, W., Lewis, S., 2016. Wave energy conversion of oscillating water column devices including air compressibility. J. Renew. Sustain. Energy 8, 054501.

SI Ocean, 2012. Ocean Energy: State of the Art. Strategic Initiative for Ocean Energy (SI Ocean). Tech. Report, Brussels, Belgium, p. 78.

SI Ocean, 2013. Ocean Energy: Cost of Energy and Cost Reduction Opportunities. Strategic Initiative for Ocean Energy (SI Ocean). Tech. Report, Brussels, Belgium, p. 29.

Simonetti, I., Cappietti, L., 2021. Hydraulic performance of oscillating water column structures as anti-reflection devices to reduce harbour agitation. Coast. Eng. 165, 103837.

Têtu, A., Fernandez-Chozas, J., 2021. A proposed guidance for the economic assessment of wave energy converters at early development stages. Energies 14, 4699.

The Carbon Trust, 2005. Oscillating Water Column Wave Energy Converter Evaluation Report. Marine Energy Challenge, p. 196.

Torre-Enciso, Y., Ortubia, I., López de Aguileta, L.I., Marqués, J., 2009. Mutriku wave power plant: from the thinking out to the reality. In: Proceedings of the 8th European Wave and Tidal Energy Conference. Uppsala, Sweden, 2009.

Torres, F.R., Teixeira, P.R.F., Didier, E., 2018. A methodology to determine the optimal size of a wells turbine in an oscillating water column device by using coupled hydro–aerodynamic models. Renew. Energy 121, 9–18.

Tsonopoulos, C., Heidman, J.L., 1990. From the virial to the cubic equation of state. Fluid Phase Equilib. 57, 261–276.

Uihlein, A., Magagna, D., 2015. Wave and tidal current energy - A review of the current state of research beyond technology. Renew. Sustain. Energy Rev. 58, 1070–1081.

Wan, C., Yang, C., Bai, X., Bi, C., Chen, H., Li, M., Jin, Y., Zhao, L., 2023. Numerical investigation on the hydrodynamics of a hybrid OWC wave energy converter combining a floating buoy. Ocean Eng. 281, 114818.

Weber, J., 2007. Representation of non-linear aero-thermodynamic effects during small scale physical modelling of OWC wecs. In: Proceedings of the 7th European Wave and Tidal Energy Conference. Porto, Portugal, p. 207.

Yang, J., Chen, B., 2016. Emergy-based sustainability evaluation of wind power generation systems. Appl. Energy 177, 239–246.